

# Localization of Radiolabeled Chemotactic Peptide at Focal Sites of *Escherichia coli* Infection in Rabbits: Evidence for a Receptor-Specific Mechanism

John W. Babich, Ronald G. Tompkins, Wendy Graham, Sandra A. Barrow and Alan J. Fischman

Division of Nuclear Medicine of the Department of Radiology, and the Trauma Service of the Department of Surgery, Massachusetts General Hospital and Shriners Burns Institute, Boston, Massachusetts

The infection imaging properties of a high-affinity  $^{99m}\text{Tc}$ -labeled chemotactic peptide receptor agonist (N-formyl-methionyl-leucyl-phenylalanine-lysine; N-For-MLFK) were compared with a low-affinity agonist (N-Acetyl-MLFK; N-Ac-MLFK), a moderate-affinity antagonist (N-isobutyloxycarbonyl-MLFK; N-iBoc-MLFK) and non-specific inflammation imaging agents. **Methods:** All peptides were prepared by solid-phase methods and purified by high-performance liquid chromatography. The products were assayed in vitro for N-formyl-methionyl-leucyl-phenylalanine receptor binding and superoxide production. Three types of studies were performed in rabbits with *Escherichia coli* infection: (Study A) Four groups of six animals were coinjected with  $^{99m}\text{Tc}$ -N-For-MLFK-hydrazinonicotinamide (N-For-MLFK-HYNIC) plus  $^{111}\text{In}$ -immunoglobulin G,  $^{111}\text{In}$ -red blood cells or  $^{111}\text{In}$ -diethylene triamine pentaacetic acid. (Study B) Three groups of six rabbits were coinjected with  $^{111}\text{In}$ -leukocytes plus  $^{99m}\text{Tc}$ -N-For-MLFK-HYNIC,  $^{99m}\text{Tc}$ -N-Ac-MLFK-HYNIC or  $^{99m}\text{Tc}$ -N-iBoc-MLFK-HYNIC. (Study C) Two groups of six rabbits were injected with  $^{99m}\text{Tc}$ -N-For-MLFK-HYNIC and  $^{111}\text{In}$ -leukocytes with and without an excess of antagonist. In all three studies, the radiopharmaceuticals were injected 24 hr after infection and dual photon ( $^{99m}\text{Tc}$  and  $^{111}\text{In}$ ) gamma camera images were acquired at 2–3 and 16–18 hr later. Target-to-background (T/B) ratios were calculated for regions of interest drawn over the infected and contralateral normal tissue. **Results:** N-For-MLFK, N-Ac-MLFK and N-iBoc-MLFK had  $\text{EC}_{50}\text{s}$  for receptor binding of 2.0, 830 and 150 nM, respectively. The corresponding  $\text{EC}_{50}\text{s}$  for superoxide production were 20.0,  $\approx 10^3$  and  $>10^4$ . Study A demonstrated that the T/B for  $^{99m}\text{Tc}$ -N-For-MLFK-HYNIC was higher than for any of the nonspecific imaging agents ( $p < 0.001$ ), and  $^{111}\text{In}$ -immunoglobulin G had a higher T/B ratio than  $^{111}\text{In}$ -diethylenetriamine pentaacetic acid ( $p < 0.01$ ) or  $^{111}\text{In}$ -red blood cells ( $p = \text{NS}$ ). Study B showed that  $^{99m}\text{Tc}$ -N-For-MLFK-HYNIC had a higher T/B ratio than the other peptides ( $p < 0.001$ ).  $^{111}\text{In}$ -leukocytes and  $^{99m}\text{Tc}$ -N-iBoc-MLFK-HYNIC had comparable T/B ratios, which were higher than for  $^{99m}\text{Tc}$ -N-Ac-MLFK-HYNIC ( $p < 0.05$ ). Study C demonstrated that coinjection with an antagonist resulted in a significant reduction in the T/B ratio for  $^{99m}\text{Tc}$ -N-For-MLFK-HYNIC ( $p < 0.001$ ), but did not affect the T/B ratio for  $^{111}\text{In}$ -leukocytes. **Conclusion:** Nonspecific mechanisms contribute minimally to the localization of  $^{99m}\text{Tc}$ -chemotactic peptide analogs at sites of infection and the majority of the accumulation appears to be receptor mediated. Also, chemotactic peptide receptor antagonists can be used for infection imaging. These results provide important new insights for future radiopharmaceutical development.

**Key Words:** agonist; antagonists; peptide; chemotactic infection

**J Nucl Med 1997; 38:1316–1322**

Leukocyte migration to focal sites of inflammation is mediated by a variety of chemoattractant signals. The tri-peptide, N-formyl-methionyl-leucyl-phenylalanine (For-MLF), is one of

the most potent chemoattractants, and a distinct class of receptors for this peptide has been identified on white blood cells (WBCs) (1–3). These receptors are present on both polymorphonuclear leukocytes (PMNs) and mononuclear phagocytes. As cells respond to the chemoattractant gradient, the affinity of the receptors decreases as additional receptors are expressed (4–6). Previous studies have demonstrated that many synthetic analogs of this peptide bind to neutrophils and macrophages with equal or greater affinity compared to the native peptide (7–9). Based on this information, we hypothesized that chemoattractant peptide analogs, which can be readily radiolabeled with radionuclides suitable for external imaging, might be effective agents for the rapid localization of focal sites of inflammation.

Recent studies in our laboratory have demonstrated that  $^{111}\text{In}$ - and  $^{99m}\text{Tc}$ -labeled For-MLF analogs retain biological and receptor binding activity and can be used for the rapid identification of focal sites of infection in rats and rabbits (7,10). In these studies, the  $^{99m}\text{Tc}$ -labeled peptides yielded images with extraordinarily high target-to-background (T/B) ratios; much higher than the values measured with coinjected  $^{111}\text{In}$ -leukocytes (8) or human polyclonal immunoglobulin G (IgG) (11). In addition, the peptides can be radiolabeled with  $^{99m}\text{Tc}$  at extremely high specific activities (12). At these specific activities excellent quality images were obtained at concentrations of peptide, which are far below the levels that produce significant reductions in peripheral leukocyte counts in rabbits or monkeys (8,12). In studies of burned rabbits with and without infection, we demonstrated that peptide localization is relatively infection selective (13).

Although these studies indicate that  $^{111}\text{In}$ - and  $^{99m}\text{Tc}$ -labeled chemotactic peptides accumulate at sites of infection with high T/B ratios, receptor specificity has not been completely established and a significant amount of localization could be due to nonspecific processes, such as increased tissue permeability, blood pool or blood flow characteristics of inflammatory lesions, or characteristics of the peptides that are not related to For-MLF receptor binding. The experiments described in this study were designed to address these issues. In these studies, New Zealand white rabbits were infected with *Escherichia coli*, coinjected with various combinations of radiopharmaceuticals and imaged 2–3 and 16–18 hr later.

## MATERIALS AND METHODS

For-MLF, N-formyl-norleucyl-leucyl-phenylalanyl-norleucyl-tyrosyl-lysine (For-Nle-LP-Nle-YK), phorbol 12-myristate 13-acetate and cytochalasin B were purchased from Sigma Chemical Co. (St. Louis, MO). For- $^3\text{H}$ MLF (60 Ci/mmol),  $^{99m}\text{TcO}_4^-$  ( $^{99}\text{Mo}/^{99m}\text{Tc}$ -generator),  $^{111}\text{In}$ -diethylene triamine pentaacetic acid (DTPA) and stannous glucoheptonate (Glucoscan) were obtained from DuPont (Billerica, MA). Indium-111-oxine was obtained from

Received Oct. 15, 1996; revision accepted Jan. 7, 1997.

For correspondence or reprints contact: Alan J. Fischman, MD, PhD, Division of Nuclear Medicine, Massachusetts General Hospital, Boston, MA 02114.

Amersham Inc. (Arlington Heights, IL). Safety-Solve was obtained from Research Products International Corp. (Mt. Prospect, IL). Hanks' balanced salt solution was from GIBCO (Grand Island, NY). Dimethylformamide, trifluoroacetic acid (TFA), ether, petroleum ether, ethyl acetate, p-cresol and p-nitro benzaldehyde were obtained from Aldrich Chemical Co. (St. Louis, MO.). Inorganic salts were obtained from Fisher Scientific Co (St. Louis, MO). Instant thin-layer silica gel chromatography (ITLC-SG) chromatographic strips were obtained from Gelman Laboratories (Ann Arbor, MI).

### Peptide Synthesis

N-formyl-methionyl-leucyl-phenylalanine-lysine (N-For-MLFK), N-acetyl-MLFK (N-Ac-MLFK) and isobutyloxycarbonyl-MLFK (iBoc-MLFK) were synthesized and purified by standard solid-phase techniques (14,15), as previously described (8-13). Hydrazinonicotinamide (HYNIC)-derivatized chemotactic peptides, N-For-MLFK-HYNIC, N-Ac-MLFK-HYNIC and iBoc-MLFK-HYNIC were prepared by reacting the  $\epsilon$  amino group of the C-terminal lysyl peptides with succinimidyl-6-t-Boc-hydrazinopyridine-3-carboxylic acid. The t-Boc group was removed by stirring the product with TFA containing p-cresol for 15 min at 20°C. The products were purified by preparative reverse-phase HPLC on a 2.5 × 50 cm Whatman ODS-3 column eluted with a gradient of water/acetonitrile in 0.1% TFA. Chemical purity was evaluated by thin-layer chromatography (TLC), high-performance liquid chromatography (HPLC), UV spectroscopy, mass spectroscopy and amino acid analysis. Further details on the preparation of HYNIC derivatized chemotactic peptides have been reported (7).

### Receptor Binding

Isolated human neutrophils (PMNs,  $8 \times 10^5$ ) were incubated in phosphate buffered saline containing 1.7 mM  $\text{KH}_2\text{PO}_4$ , 8.0 mM  $\text{Na}_2\text{HPO}_4$ , 0.117 M NaCl, 0.15 mM  $\text{CaCl}_2$ , 0.5 mM  $\text{MgCl}_2$  and 1.0 mM phenylmethylsulfonyl fluoride (pH 7.4) (incubation buffer) at 24°C for 45 min in a total volume of 0.15 ml in the presence and absence of increasing concentrations of test peptide and 15 nM For- $^3\text{H}$ -MLF (16). The cells were then filtered onto glass fiber disks and washed with 20 ml of ice-cold incubation buffer. The filters were placed in scintillation vials with 10 ml of Safety-Solve and cell-associated radioactivity was measured by liquid scintillation spectroscopy. Specific binding was defined as total minus nonspecific binding. Nonspecific binding was defined as the amount of residual radioactivity bound in the presence of 10 mM unlabeled For-MLF and was  $\approx 10\%$  of total binding.

### Superoxide Release

Superoxide release by human PMN's was measured by monitoring superoxide dismutase-inhibitable reduction of ferricytochrome C (extinction coefficient: 29.5/mmol/liter/cm) as previously (17). Briefly, isolated human cells were incubated with Hanks' balanced salt solution alone or with increasing concentrations of the peptide analogs, For-MLF or For-Nle-LP-Nle-YK (range: 1 nM to 1 mM) in the presence of 10 mM cytochalasin B plus or minus superoxide dismutase (50 mg/ml) at 37°C for 10 min followed by spectrophotometric measurement of ferricytochrome C reduction.

### Radiopharmaceutical Preparation

**Technetium-99m-Labeled Chemotactic Peptides.** A  $^{99\text{m}}\text{Tc}$  generator was eluted  $\approx 5$  hr after a previous elution to yield  $\approx 500$  mCi of  $^{99\text{m}}\text{TcO}_4^-$ . A typical elution contained  $\approx 3$  nM of  $^{99\text{m}}\text{Tc}$ ; the  $^{99\text{m}}\text{Tc}$  to  $^{99\text{m}}\text{Tc}$  ratio was  $\approx 1.5:1$  and specific activity was  $> 100,000$  mCi/ $\mu\text{mol}$ . Technetium-99m-glucoheptonate ( $^{99\text{m}}\text{Tc}$ -Gluco) was used to provide the Tc(V) oxo species for radiolabeling HYNIC-conjugated peptides (18). Technetium-99m-gluco was prepared by adding  $\approx 300$  mCi of  $^{99\text{m}}\text{TcO}_4^-$  in saline ( $\approx 2.5$  ml) to freeze-dried

kits. The radiochemical purity of the product was  $>95\%$  by ITLC-sg using both acetone and saline as mobile phase solvents.

The HYNIC-derivatized chemotactic peptides ( $\approx 200$   $\mu\text{g}$ ), were dissolved in 200  $\mu\text{l}$  of dimethyl sulfoxide and diluted to 20  $\mu\text{g}/\text{ml}$  with 50 mM acetate buffer, pH 5.2. The peptide solution (0.5 ml) was placed in a clean glass vial,  $^{99\text{m}}\text{Tc}$ -gluco (0.5 ml,  $\approx 75$  mCi) was added and the mixture was vortexed and allowed to stand at room temperature for 1 hr. Peptide labeling was monitored by ITLC-sg using three solvent systems: acetone, saline and acetone: water (9:1). Radiolabeled peptide was purified by reverse-phase HPLC on a C-18 column (5  $\mu$ , 4.5 × 46 mm) eluted with a binary gradient (solvent A, 0.1% TFA in water; solvent B, 0.1% TFA in acetonitrile; Gradient, 0%–100% B over 20 min). Specific activity was calculated using the relation (% radiochemical yield × mCi present)/(mmol of peptide × 100%).

**Indium-111-Labeled Human Polyclonal IgG.** Human polyclonal IgG was derivatized with DTPA by means of the DTPA-carboxy-carbonic anhydride chelate method (19,20). Approximately two chelating groups were present per IgG. The conjugate was radiolabeled with  $^{111}\text{In}$ - by a previously reported method (21,22). Radiochemical purity was determined using ITLC-SG chromatographic strips developed with 0.1 M sodium citrate (pH 5.5); typically,  $>90\%$  of the radioactivity was associated with antibody.

**Indium-111-Labeled Leukocytes.** Approximately 20 ml of heparinized blood was drawn from an ear artery of the infected rabbits, diluted 1:1 with Hespan and leukocytes were isolated by a previously described procedure (23,24) with the following modifications. The blood was sedimented for 45 min and leukocyte-rich plasma (LRP) was isolated. The LRP was centrifuged at 450 × g for 5 min and the leukocyte pellet was suspended in saline (10 ml) and allowed to stand at room temperature for 1 hr. The supernatant was removed and the cells were resuspended in fresh saline (5 ml). Indium-111-oxine (500  $\mu\text{Ci}$ ) was added dropwise with agitation and the mixture was incubated at 37°C for 1 hr with intermittent agitation. The radiolabeled cells were allowed to sediment and the pellet was suspended in platelet poor plasma.

**Indium-111-Labeled Red Blood Cells (RBCs).** Approximately 5 ml of heparinized blood was drawn from an ear artery of the infected rabbits and centrifuged for 5 min at 1000 × g. The cells were washed with saline (10 ml, 3 times) and radiolabeled with  $^{111}\text{In}$ -oxine (500  $\mu\text{Ci}$ ) as described above.

**Infection Model.** Male New Zealand white rabbits weighing 3.5–4.0 kg were used in all studies. *E. coli* from a single clinical isolate were grown overnight on trypticase soy agar plates and individual colonies were diluted with sterile normal saline to produce a turbid suspension containing about  $2 \times 10^{11}$  organisms per ml. Radiopharmaceuticals were administered 24 hr after bacterial injection, when the animals were judged to have moderate infections by palpation.

### Radiopharmaceutical Injection and Imaging Protocols

**Comparison of Technetium-99m-N-For-MLFK-HYNIC with Non-specific Agents.** In this study the infection imaging properties of  $^{99\text{m}}\text{Tc}$ -N-For-MLFK-HYNIC (specific activity  $> 10,000$  mCi/ $\mu\text{mol}$ ) were compared with  $^{111}\text{In}$ -DTPA,  $^{111}\text{In}$ -RBCs and  $^{111}\text{In}$ -IgG. Although radiolabeled DTPA and RBCs are not very useful clinically for abscess localization, they are valuable controls for the increases in tissue permeability and hyperemia that are present at inflammatory lesions. For these studies, groups of rabbits (n = 6) were injected with the following combinations of radiopharmaceuticals:

Group 1: 0.5 mCi of  $^{99\text{m}}\text{Tc}$ -N-For-MLFK-HYNIC + 0.05 mCi of  $^{111}\text{In}$ -DTPA.

Group 2: 0.5 mCi of  $^{99\text{m}}\text{Tc}$ -N-For-MLFK-HYNIC + 0.05 mCi of  $^{111}\text{In}$ -IgG.

Group 3: 0.5 mCi of  $^{99m}\text{Tc-N-For-MLFK-HYNIC}$  + 0.05 mCi of  $^{111}\text{In-RBCs}$ .

*Comparison of Technetium-99m-N-For-MLFK-HYNIC with a Low-Affinity Chemotactic Peptide Receptor Agonist and an Antagonist.* In this study the infection imaging properties of  $^{99m}\text{Tc-N-For-MLFK-HYNIC}$  were compared with  $^{111}\text{In-WBCs}$ ,  $^{99m}\text{Tc-N-Ac-MLFK-HYNIC}$  (a low-affinity agonist) and  $^{99m}\text{Tc-iBoc-MLFK-HYNIC}$  (a moderate-affinity antagonist). Radiolabeled leukocytes were injected through a marginal ear vein and 5 min later  $^{99m}\text{Tc}$ -labeled peptide (specific activity > 10,000 Ci/mmol) was injected in the opposite ear. The radiolabeled WBCs served as a reference for verifying uniformity of infection intensity between animals and experimental groups. The following combinations of radiopharmaceuticals were studied:

Group 1: 0.5 mCi of  $^{99m}\text{Tc-N-For-MLFK-HYNIC}$  + 0.05 mCi of  $^{111}\text{In-WBCs}$ .

Group 2: 0.5 mCi of  $^{99m}\text{Tc-N-Ac-MLFK-HYNIC}$  + 0.05 mCi of  $^{111}\text{In-WBCs}$ .

Group 3: 0.5 mCi of  $^{99m}\text{Tc-iBoc-MLFK-HYNIC}$  + 0.05 mCi of  $^{111}\text{In-WBCs}$ .

*Blockade of  $^{99m}\text{Tc-N-For-MLFK-HYNIC}$  Localization by a Chemotactic Peptide Antagonist.* In this study the effect of coinjection of a chemotactic peptide antagonist on the infection imaging properties of  $^{99m}\text{Tc-N-For-MLFK-HYNIC}$  was evaluated. All animals were coinjected with  $^{111}\text{In-WBCs}$ . Radiolabeled leukocytes were injected through a marginal ear vein and 5 min later  $^{99m}\text{Tc}$ -labeled peptide (specific activity > 10,000 mCi/ $\mu\text{mol}$ ) was injected in the opposite ear. The radiolabeled WBCs served as a reference standard for normalization of the peptide T/B ratios. The following groups of rabbits were studied:

Group 1: 0.5 mCi of  $^{99m}\text{Tc-N-For-MLFK-HYNIC}$  + 0.05 mCi of  $^{111}\text{In-WBCs}$ .

Group 2: 0.5 mCi of  $^{99m}\text{Tc-N-For-MLFK-HYNIC}$  + 0.05 mCi of  $^{111}\text{In-WBCs}$  + 1.0 mg of N-iBoc-MLFK.

### Gamma Camera Imaging and Biodistribution

At 2–3 and 16–18 hr following injection of the radiopharmaceuticals, the animals were anesthetized with ketamine/xylazine (15.0 and 1.5 mg/kg) and anterior images were acquired using a large field-of-view gamma camera equipped with a parallel hole medium energy collimator. Indium-111 and  $^{99m}\text{Tc}$  images were acquired simultaneously with 15% windows centered on photo peaks at 140 KeV for  $^{99m}\text{Tc}$  and 247 KeV for  $^{111}\text{In}$ . Phantom studies were performed to calculate the amount of cross-over of 174 KeV photons of  $^{111}\text{In}$  into the  $^{99m}\text{Tc}$  window and these data were used to correct the  $^{99m}\text{Tc}$  images. Regions-of-interest were drawn over the area of infection and the contralateral normal muscle and T/B ratios were calculated. After acquiring the final images, the animals were killed with an overdose of sodium pentobarbital. The lesions were carefully dissected and 5–6 representative samples of infected muscle ( $\approx 1$  g each) without associated pus were excised. Samples of uninfected muscle were excised from contralateral thigh muscle. Regions with purulent exudate were localized and samples of pus were removed with the blunt edge of a scalpel. The concentrations of radioactivity in the samples of tissue and pus was measured with a well scintillation gamma counter. For comparison with the imaging results, infected-to-normal muscle and pus-to-normal muscle ratios were calculated.

### Statistical Analysis

The results of the imaging and biodistribution studies were evaluated statistically by ANOVA followed by Duncan's new multiple range test (25). For the studies comparing the imaging properties of  $^{99m}\text{Tc-For-MLFK-HYNIC}$  with nonspecific agents or other peptides and  $^{111}\text{In-WBCs}$  (Studies 1 and 2), two-way ANOVA with a linear model in which time after injection and

**TABLE 1**  
EC<sub>50</sub>s for For-MLF Receptor Binding and Superoxide Generation

Peptide	Receptor Binding (EC <sub>50</sub> , nM)	SO* release (EC <sub>50</sub> , nM)	Peptide class
N-For-MLFK	2.0	20.0	Agonist
N-Ac-MLFK	830	$\sim 10^3$	Weak agonist
N-iBoc-MLFK	150	$> 10^4$	Weak antagonist

\*Superoxide.

radiopharmaceutical were the classification variables used: T/B = Time + Radiopharmaceutical + Time  $\times$  Radiopharmaceutical. For evaluating the effect of a chemotactic peptide antagonist on  $^{99m}\text{Tc-For-MLFK-HYNIC}$  localization, the T/B ratios  $^{99m}\text{Tc-For-MLFK-HYNIC}$  in the presence and absence of antagonist were divided by the corresponding ratios for  $^{111}\text{In-WBCs}$  and the normalized values were analyzed by two-way ANOVA with the same linear model. For the biodistribution data, one-way ANOVA with radiopharmaceutical as the classification variable was used. All results were expressed as mean  $\pm$  s.e.m.

## RESULTS

### Peptide Synthesis, Radiolabeling and in Vitro Characterization

The chemotactic peptides and their hydrazino nicotinamide derivatives were prepared in good yield and excellent chemical purity (>98%). All products were homogeneous on both TLC and HPLC. UV analysis showed maximum absorption bands at 268 and 315 nm. Amino acid and mass spectral analyses were consistent with the expected products. When radiolabeled with  $^{99m}\text{Tc}$ , typical specific activities were >10,000 mCi/ $\mu\text{mol}$  after HPLC purification. EC<sub>50</sub>s for binding to the chemoattractant receptor on human PMNs and superoxide generation are summarized in Table 1. No adverse effects were detected after intravenous administration of any of the peptides in the animals studied.

### Comparison of Technetium-99m-N-For-MLFK-HYNIC with Nonspecific Agents

In this study the infection imaging properties of  $^{99m}\text{Tc-N-For-MLFK-HYNIC}$  were compared with  $^{111}\text{In-DTPA}$ ,  $^{111}\text{In-RBCs}$  and  $^{111}\text{In-IgG}$  in groups of six rabbits. Figure 1 shows representative gamma camera images for all four radiopharmaceuticals  $\approx 17$  hr after injection. These data clearly indicate that infection localization was best with the  $^{99m}\text{Tc}$ -labeled peptide. However, significant accumulations of  $^{111}\text{In-IgG}$  and  $^{111}\text{In-RBCs}$  were also detected. In contrast, at this imaging time, minimal accumulation of  $^{111}\text{In-DTPA}$  was observed.

Figure 2A summarizes the T/B ratios 2–3 and  $\approx 17$  hr after injection for all animals studied. ANOVA demonstrated significant main effects of radiopharmaceutical ( $p < 0.001$ ), time ( $p < 0.001$ ) and radiopharmaceutical by time interaction ( $p < 0.001$ ). Equivalence of the infections in all groups of animals was validated by inspection of the lesions after death and the fact that the T/B ratios for the  $^{99m}\text{Tc}$ -labeled peptide in Groups 1–3 were nearly identical ( $p = \text{ns}$ , data not shown). At both imaging times,  $^{99m}\text{Tc-N-For-MLFK-HYNIC}$  had a higher T/B ratio than any other agent ( $p < 0.001$ ) and the ratio increased significantly between early and delayed imaging ( $p < 0.01$ ). Indium-111 IgG had a significantly higher T/B ratio than  $^{111}\text{In-DTPA}$  ( $p < 0.05$ ) and a slightly higher T/B ratio than  $^{111}\text{In-RBCs}$  ( $p = \text{ns}$ ). Between early and delayed imaging, the T/B ratios for  $^{111}\text{In-IgG}$  and  $^{111}\text{In-RBCs}$  increased slightly; how-

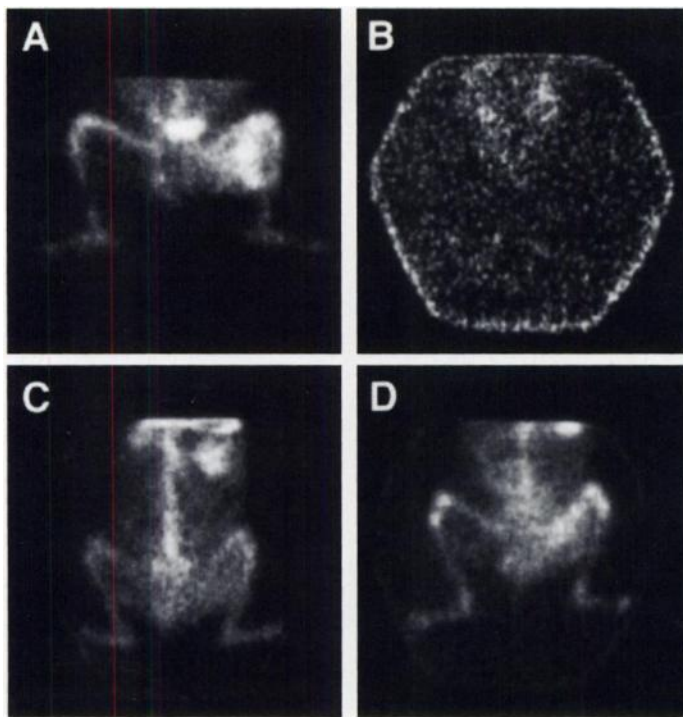


**FIGURE 1.** Representative gamma camera images (anterior) of rabbits with *E. coli* infection of the left thigh 17 hr after injection of:  $^{99m}\text{Tc}$ -N-For-MLFK-HYNIC (A),  $^{111}\text{In}$ -DTPA (B),  $^{111}\text{In}$ -RBCs (C) and  $^{111}\text{In}$ -IgG (D).

ever, the differences were not significant. For  $^{111}\text{In}$ -DTPA, T/B was similar for early and delayed imaging ( $p = \text{NS}$ ).

Figure 2B summarizes the infected-to-normal muscle and pus-to-normal muscle T/B ratios determined by direct radioactivity measurements on samples of excised tissue. Absolute tissue concentrations are shown in Table 2. For both ratios, ANOVA demonstrated highly significant main effects of radiopharmaceutical ( $p < 0.0001$ ) and  $^{99m}\text{Tc}$ -N-For-MLFK-HYNIC

had higher T/B than any of the other agents tested ( $p < 0.01$ ). The T/B for  $^{111}\text{In}$ -IgG was significantly higher than the ratios for  $^{111}\text{In}$ -DTPA ( $p < 0.01$ ) and  $^{111}\text{In}$ -RBCs ( $p < 0.05$ ). The T/B for  $^{111}\text{In}$ -RBCs was significantly higher than the ratio for  $^{111}\text{In}$ -DTPA ( $p < 0.05$ ).

#### Comparison of Technetium-99m-N-For-MLFK-HYNIC with a Low-Affinity Chemotactic Peptide Receptor Agonist and an Antagonist

In this study, the infection imaging properties of  $^{99m}\text{Tc}$ -N-For-MLFK-HYNIC were compared with  $^{99m}\text{Tc}$ -N-Ac-MLFK-HYNIC [a low-affinity chemotactic peptide agonist,  $\text{EC}_{50}$  (superoxide)  $> 1.0 \text{ mM}$ ,  $\text{EC}_{50}$  (receptor binding) =  $830 \text{ nM}$ ] and  $^{99m}\text{Tc}$ -N-iBoc-MLFK-HYNIC [a moderate-affinity receptor antagonist,  $\text{EC}_{50}$  (superoxide)  $> 10.0 \text{ mM}$ ,  $\text{EC}_{50}$  (receptor binding) =  $150 \text{ nM}$ ]. All animals were coinjected with  $^{111}\text{In}$ -WBCs.

Figure 3 shows representative gamma camera images for all four radiopharmaceuticals  $\approx 17 \text{ hr}$  after injection. These data indicate that infection localization was best with  $^{99m}\text{Tc}$ -N-For-MLFK-HYNIC. The next highest level of accumulation was detected with  $^{99m}\text{Tc}$ -N-iBoc-MLFK-HYNIC and  $^{111}\text{In}$ -WBCs. Low levels of accumulation were observed with  $^{99m}\text{Tc}$ -N-Ac-MLFK-HYNIC

Figure 4A summarizes the T/B ratios 2–3 and  $\approx 17 \text{ hr}$  after injection for all animals that were studied. ANOVA demonstrated significant main effects of radiopharmaceutical ( $p < 0.001$ ), time ( $p < 0.001$ ) and radiopharmaceutical by time interaction ( $p < 0.001$ ). Equivalence of the infections in all groups of animals was validated by inspection of the lesions after death and the fact that the T/B ratios for  $^{111}\text{In}$ -WBCs in groups 1–3 were nearly identical (data not shown). At both imaging times,  $^{99m}\text{Tc}$ -N-For-MLFK-HYNIC had a higher T/B ratio than for any other agent ( $p < 0.001$ ) and the ratio increased significantly between early and delayed imaging ( $p < 0.01$ ). Indium-111-WBCs and the moderate-affinity antagonist had comparable T/Bs, which were higher than the low-affinity

**FIGURE 2.** (A) T/B ratios for rabbits with *E. coli* infection 2–3 hr (open bars) and 16–18 hr (solid bars) after injection of  $^{99m}\text{Tc}$ -N-For-MLFK-HYNIC,  $^{111}\text{In}$ -IgG,  $^{111}\text{In}$ -RBCs and  $^{111}\text{In}$ -DTPA. (B) Corresponding infected-to-normal muscle ratios (open bars) and pus-to-normal muscle ratios (solid bars) determined by tissue radioactivity measurements after death. The animals were infected 24 hr before radiopharmaceutical injection. Each value is the mean  $\pm$  s.e.m. for six animals.

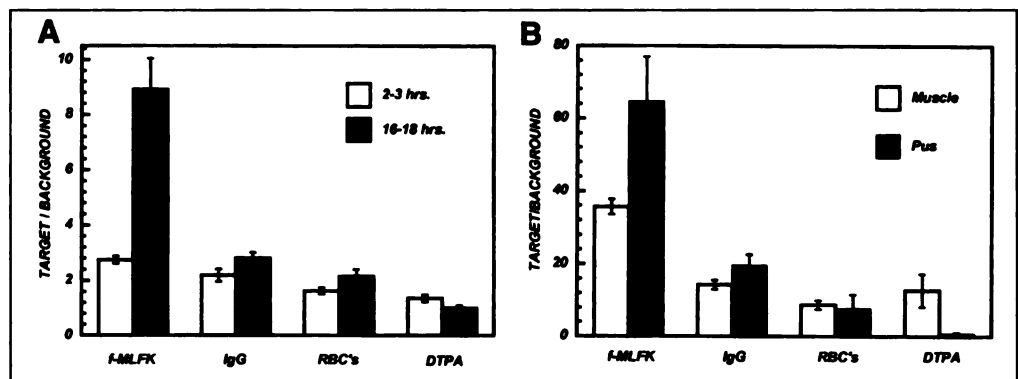


**TABLE 2**

Concentrations (%ID/g) of Nonspecific Imaging Agents and Chemotactic Peptide Analogs in Normal Muscle, Infected Muscle and Pus

Agent	Normal muscle	Infected muscle	Pus
DTPA	0.0034 $\pm$ 0.00036	0.0041 $\pm$ 0.0015	0.0021 $\pm$ 0.00058
RBCs	0.0038 $\pm$ 0.00073	0.030 $\pm$ 0.0031	0.025 $\pm$ 0.0094
IgG	0.0016 $\pm$ 0.00067	0.023 $\pm$ 0.0045	0.030 $\pm$ 0.013
WBCs	0.0038 $\pm$ 0.0011	0.024 $\pm$ 0.0018	0.035 $\pm$ 0.0076
N-For-MLFK	0.0030 $\pm$ 0.00044	0.10 $\pm$ 0.0084	0.18 $\pm$ 0.034
N-iBoc-MLFK	0.0025 $\pm$ 0.00055	0.048 $\pm$ 0.010	0.089 $\pm$ 0.040
N-Ac-MLFK	0.0054 $\pm$ 0.00025	0.033 $\pm$ 0.0020	0.045 $\pm$ 0.0082

DTPA = diethylene triamine pentaacetic acid; RBC = red blood cell; IgG = immunoglobulin G; WBC = White blood cell.

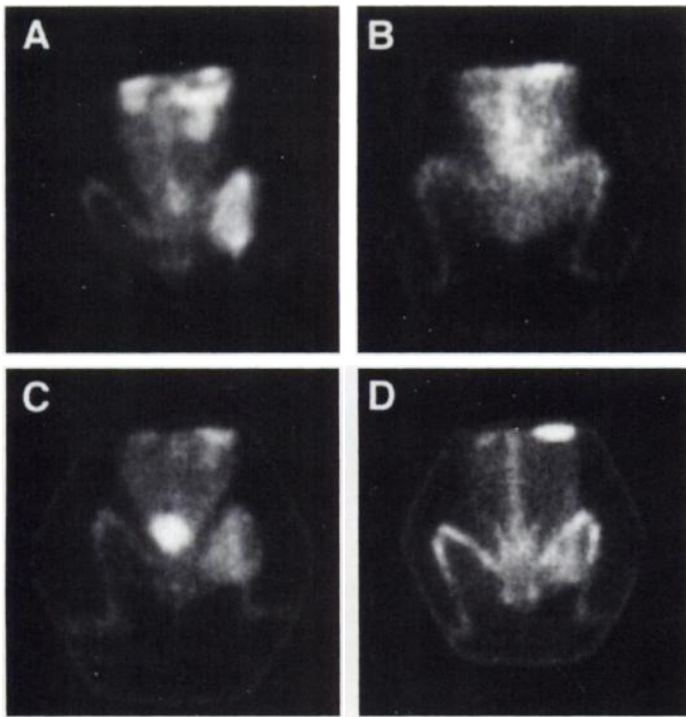


**FIGURE 3.** Representative gamma camera images (anterior) of rabbits with *E. coli* infection of the left thigh 17 hr after injection of:  $^{99m}\text{Tc}$ -N-For-MLFK-HYNIC (A),  $^{99m}\text{Tc}$ -N-Ac-MLFK-HYNIC (B),  $^{99m}\text{Tc}$ -iBoc-MLFK-HYNIC (C) and  $^{111}\text{In}$ -WBCs (D).

agonist ( $p < 0.05$ ). For  $^{111}\text{In}$ -WBCs and  $^{99m}\text{Tc}$ -N-iBoc-MLFK-HYNIC, T/B increased between the early and delayed images ( $p < 0.05$ ). In contrast, with  $^{99m}\text{Tc}$ -N-Ac-MLFK-HYNIC, T/B did not change significantly between the two imaging times ( $p = \text{ns}$ ). In other studies, it was demonstrated that  $^{99m}\text{Tc}$ -N-Ac-MLFK-HYNIC and  $^{99m}\text{Tc}$ -N-iBoc-MLFK-HYNIC had no effect on peripheral leukocyte levels even at high doses (data not shown).

Figure 4B summarizes the infected-to-normal muscle and pus-to-normal muscle T/B ratios determined by direct radioactivity measurements on samples of excised tissue. Absolute tissue concentrations are shown in Table 2. For both ratios, ANOVA demonstrated a highly significant main effect of radiopharmaceutical ( $p < 0.0001$ ). The infected-to-normal muscle ratio for  $^{99m}\text{Tc}$ -N-For-MLFK-HYNIC was higher than the T/B ratio for any of the other agents ( $p < 0.01$ ), and T/B for  $^{99m}\text{Tc}$ -N-iBoc-MLFK-HYNIC was higher than the ratios for N-Ac-MLFK-HYNIC ( $p < 0.01$ ) and  $^{111}\text{In}$ -WBCs ( $p < 0.01$ ). The pus-to-normal muscle ratio for  $^{99m}\text{Tc}$ -N-For-MLFK-HYNIC was significantly higher than the ratios for N-Ac-MLFK-HYNIC ( $p < 0.01$ ) and  $^{111}\text{In}$ -WBCs ( $p < 0.01$ ). The ratio for N-iBoc-MLFK-HYNIC was significantly

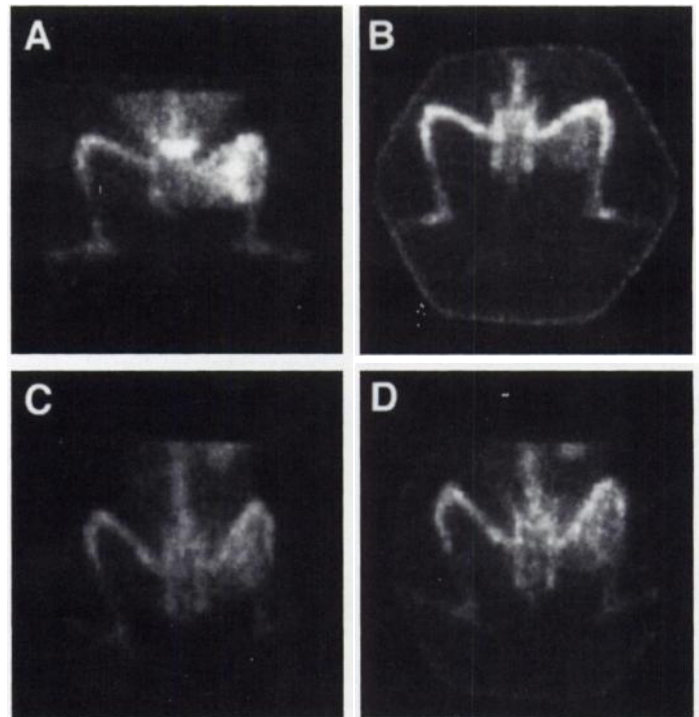


**FIGURE 5.** Representative gamma camera images (anterior) of rabbits with *E. coli* infection of the left thigh 17 hr after injection of  $^{99m}\text{Tc}$ -N-For-MLFK-HYNIC alone (A) and with the antagonist (C). Corresponding  $^{111}\text{In}$ -WBC images are also shown (B,D).

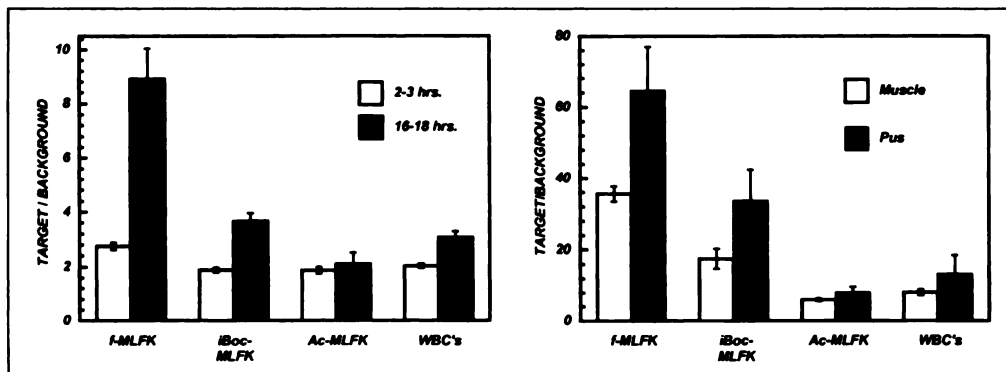
higher than the ratios for N-Ac-MLFK-HYNIC ( $p < 0.05$ ) and  $^{111}\text{In}$ -WBCs ( $p < 0.05$ ).

#### Blockade of Technetium-99m-N-For-MLFK-HYNIC Localization by a Chemotactic Peptide Antagonist

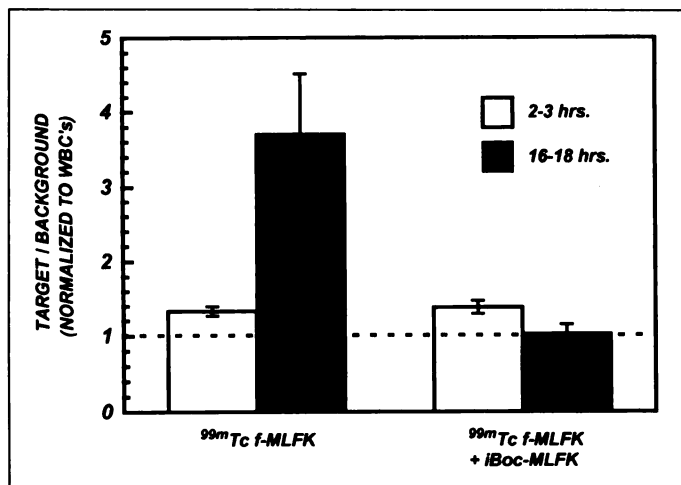
In this study the effect of coinjection of a chemotactic peptide antagonist on the infection imaging properties of  $^{99m}\text{Tc}$ -N-For-MLFK-HYNIC was evaluated. All animals were coinjected with  $^{111}\text{In}$ -WBCs.

Figure 5 shows representative gamma camera images for Group 1 and 2 animals  $\approx 17$  hr after injection. These data indicate that accumulation of  $^{99m}\text{Tc}$ -N-For-MLFK-HYNIC at the site of infection was significantly reduced by coinjection of a large dose of antagonist. In contrast, the antagonist did not have a significant effect on localization of  $^{111}\text{In}$ -WBCs.

Figure 6 summarizes the T/B 2–3 and  $\approx 17$  hr after injection for all animals studied. ANOVA demonstrated significant main effects of radiopharmaceutical ( $p < 0.001$ ), time ( $p < 0.05$ ) and radiopharmaceutical by time interaction ( $p < 0.001$ ). At the early imaging time, coinjection of the antagonist did not have a significant effect on peptide localization. In contrast, a marked reduction in accumulation was observed at the late imaging



**FIGURE 4.** (Left) T/B ratios for rabbits with *E. coli* infection 2–3 hr (open bars) and 16–18 hr (solid bars) after injection of  $^{99m}\text{Tc}$ -N-For-MLFK-HYNIC,  $^{99m}\text{Tc}$ -iBoc-MLFK-HYNIC,  $^{99m}\text{Tc}$ -N-Ac-MLFK-HYNIC and  $^{111}\text{In}$ -WBCs. (Right) Corresponding infected-to-normal muscle ratios (open bars) and pus-to-normal muscle ratios (solid bars) determined by tissue radioactivity measurements after death. The animals were infected 24 hr before radiopharmaceutical injection. Each value is the mean  $\pm$  s.e.m. for six animals.



**FIGURE 6.** T/B ratios for rabbits with *E. coli* infection 2–3 hr (open bars) and 16–18 hr (solid bars) after injection of  $^{99m}\text{Tc}$ -N-For-MLFK-HYNIC alone and with the antagonist. The animals were infected 24 hr before radiopharmaceutical injection. Each value is the mean  $\pm$  s.e.m. for six animals.

time ( $p < 0.001$ ). Coinjection of the antagonist did not have a significant effect on localization of  $^{111}\text{In}$ -WBCs at either imaging time ( $p = \text{ns}$ ).

## DISCUSSION

Indium-111- and  $^{99m}\text{Tc}$ -labeled chemotactic peptides have been shown to be among the most promising new radiopharmaceuticals for infection imaging (7,8,10–13). In previous imaging studies with these reagents, it was assumed that the mechanism of infection/inflammation localization is mediated by high-affinity binding to For-MLF receptors on leukocytes. Although most of the imaging results have been consistent with this mechanism, direct proof has not been available. In this study, we have advanced the peptide–receptor interaction hypothesis to a more rigorous theoretical basis.

The results of the studies comparing a potent  $^{99m}\text{Tc}$ -labeled chemotactic peptide agonist with agents that accumulate at inflammatory sites by nonspecific mechanisms clearly indicate that these processes make at most a minimal contribution to overall peptide localization. From the imaging studies, the degree of localization of the four agents could be ordered as follows:  $^{99m}\text{Tc}$ -peptide  $\gg$   $^{111}\text{In}$ -IgG  $>$   $^{111}\text{In}$ -RBC  $\gg$   $^{111}\text{In}$ -DTPA. The biodistribution demonstrated a similar pattern of pus-to-normal tissue ratios. In contrast, the infected-to-normal tissue ratio for  $^{111}\text{In}$ -DTPA was greater than  $^{111}\text{In}$ -RBCs and similar to  $^{111}\text{In}$ -IgG. However, this difference was not considered to be of importance because absolute accumulation was extremely low (Table 2).

The imaging and biodistribution studies with a low-affinity agonist (N-Ac-MLFK) and a moderate-affinity antagonist (N-iBoc-MLFK) lend further support to a receptor-mediated mechanism for peptide localization. It is of interest that the  $\text{EC}_{50}$  for For-MLF receptor binding of N-Ac-MLFK is considerably lower than the previously reported value for N-Ac-MLF (3). This difference could be related to the difference in net charge on the peptide and requires further investigation. Despite the fact that only a limited number of compounds were studied, the results clearly indicate that there is a correlation between T/B ratio at infection sites and affinity for For-MLF receptors on leukocytes ( $1/\text{EC}_{50}$ ). In the future, studies with agonists and antagonists with a wider range of  $\text{EC}_{50}$ s will be useful for further confirmation of this correlation. The greater magnitude of the pus-to-infected muscle ratios compared with infected-to-normal muscle ratios for all of the peptides (similar to  $^{111}\text{In}$ -

WBCs) is further evidence for WBC-mediated localization. The most compelling evidence for receptor-mediated localization are the results of the blocking studies. These investigations clearly established that coinjection of a large excess of unlabeled antagonist with a potent  $^{99m}\text{Tc}$ -labeled chemotactic peptide results in a significant reduction in T/B for peptide localization but does not have a significant effect on T/B for  $^{111}\text{In}$ -leukocytes. Autoradiographic studies might be useful to demonstrate displacement at the cellular level.

The fact that these studies were performed with a rabbit model of focal infection suggests the need for some caution in interpreting the results. Previous studies have demonstrated that rabbit and rodent leukocytes have different pharmacokinetic properties than human cells. Although it is true that T/B ratios for  $^{111}\text{In}$ -WBCs tend to be lower in infections in rabbits compared with infections of comparable severity in dogs, we have demonstrated that the overall patterns of  $^{99m}\text{Tc}$ -peptide accumulation are similar in rabbits and dogs (26). These data indicate that the rabbit model is a useful preparation for initial screenings of new reagents. Clearly, when an optimal reagent is developed, further studies in dogs or monkeys should be performed.

Overall, the results of these studies establish three important points:

1. The increased tissue permeability and blood volume of inflammatory lesions cannot explain the degree of infection localization observed with radiolabeled chemotactic peptides. Also, previous results from our laboratory have demonstrated that increased blood flow is not an important factor (27).
2. The infection localization properties of chemotactic peptides are related to the affinity for For-MLF receptor binding.
3. Receptor antagonists localize at sites of infection to a significant degree. If high-affinity antagonists are developed, they could be the optimal infection imaging agents.

Our imaging studies with a  $^{99m}\text{Tc}$ -labeled receptor antagonist is the first demonstration of infection imaging with a chemotactic peptide analog that lacks biological activity. Although the  $\text{EC}_{50}$  of the peptide analog that was tested may not be optimal for clinical imaging, the observation is extremely important since it opens a new pathway for development of convenient reagents for clinical imaging. Previously, we demonstrated that potent chemotactic peptide agonists could be radiolabeled at specific activities that result in doses of unlabeled peptide that are well below the concentrations that induce significant reduction in peripheral leukocyte levels in rabbits, dogs or monkeys (9,12,27). However, these radiolabeling procedures are relatively complex and require controlled generator elution and HPLC purification. Clearly, elimination of these requirements would be of great value for the widespread application of chemotactic peptide-based infection imaging reagents. In addition to the development of antagonists, another factor that can affect the imaging properties of chemotactic peptide infection imaging agents is the choice of the coligand that is used for radiolabeling. Although the choice of coligand has not been shown to effect receptor binding or biological activity, it can have profound influences on the pattern biodistribution to uninfected tissues (28). Currently, one of the main focuses of research in our laboratory is the development of high-affinity antagonist/coligand combinations.

## CONCLUSION

We have demonstrated that nonspecific mechanisms contribute minimally to the localization of  $^{99m}\text{Tc}$ -chemotactic peptide analogs at sites of infection and the majority of accumulation appears to be receptor mediated. Also, we have demonstrated that chemotactic peptide receptor antagonists can be used for infection imaging. These results put the receptor hypothesis for chemotactic peptide localization on firmer theoretical ground and provide important new insights for the future development of improved radiopharmaceuticals.

## ACKNOWLEDGMENT

This work was supported in part by National Institutes of Health grants 5P50 GM21700 and RO1 A131094.

## REFERENCES

1. Showell HJ, Freer RJ, Zigmund SH, Schiffmann E, Aswanikumar S, Corcoran B, Becker EL. The structural relations of synthetic peptides as chemotactic factors and inducers of lysosomal enzyme secretion for neutrophils. *J Exp Med* 1976;143:1154-1169.
2. Schiffmann E, Corcoran BA, Wahl SM. Formylmethionyl peptides as chemoattractants for leukocytes. *Proc Natl Acad Sci USA* 1975;72:1059-1062.
3. Williams LT, Snyderman R, Pike MC, Lefkowitz RJ. Specific receptor sites for chemotactic peptides on human polymorphonuclear leukocytes. *Proc Natl Acad Sci USA* 1977;74:1204-1208.
4. Snyderman R, Verghese MW. Leukocyte activation by chemoattractant receptors: roles of a guanine nucleotide regulatory protein and polyphosphoinositide metabolism. *Rev Infect Dis* 1987;9:S562-S569.
5. Fletcher MP, Seligman BE, Gallin JI. Correlation of human neutrophil secretion, chemoattractant receptor mobilization and enhanced functional capacity. *J Immunol* 1988;128:941-948.
6. Niedel J, Wilkinson S, Cuatrecasas P. Receptor mediated uptake and degradation of  $^{125}\text{I}$ -chemotactic peptide by human neutrophils. *J Biol Chem* 1979;10:700-710.
7. Babich JW, Solomon H, Pike MC, et al. Technetium-99m-labeled hydrazino nicotinamide derivatized chemotactic peptides for imaging focal sites of bacterial infection. *J Nucl Med* 1993;34:1964-1974.
8. Babich JW, Graham W, Barrow SA, Dragotakes SC, Tompkins RG, Rubin RH, Fischman AJ. Technetium-99m-labeled chemotactic peptides: comparison with indium-111-labeled white blood cells for localizing acute bacterial infections in rabbits. *J Nucl Med* 1993;34:2176-2181.
9. Niedel J, Davis J, Cuatrecasas P. Covalent affinity labeling of the formyl peptide chemotactic receptor. *J Biol Chem* 1980;255:7063-7066.
10. Fischman AJ, Pike MC, Kroon D, et al. Imaging of focal sites of bacterial infection in rats with indium-111-labeled chemotactic peptide analogs. *J Nucl Med* 1991;32:483-491.
11. Babich JW, Graham W, Barrow SA, Fischman AJ. Comparison of the infection imaging properties of a  $^{99m}\text{Tc}$ -labeled chemotactic peptide with  $^{111}\text{In}$  IgG. *Nucl Med Biol* 1995;22:643-648.
12. Fischman AJ, Rauh D, Solomon H, et al. In vivo bioactivity and biodistribution of chemotactic peptide analogs in non-human primates. *J Nucl Med* 1993;34:2130-2134.
13. Fischman AJ, Babich JW, Barrow SA, Graham W, Carter E, Tompkins RG, Rubin RH. Detection of acute bacterial infections within soft tissue injuries using a  $^{99m}\text{Tc}$ -labeled chemotactic peptide. *J Trauma* 1995;38:223-227.
14. Merrifield RB. Solid phase peptide synthesis: I. synthesis of a tetrapeptide. *J Am Chem Soc* 1963;15:2149-2154.
15. Stewart JM, Young JD. *Solid phase peptide synthesis*. San Francisco, CA: W.H. Freeman & Company; 1969.
16. Pike MC, Snyderman R. Leukocyte chemoattractant receptors. *Methods Enzymol* 1988;162:236-245.
17. Ike MC, Jakoi L, McPhail LC, Snyderman R. Chemoattractant-mediated stimulation of the respiratory burst in human polymorphonuclear leukocytes may require appearance of protein kinase activity in the cells' particulate fraction. *Blood* 1986;67:909-913.
18. Abrams MJ, Juweid M, tenKate CI, et al. Technetium-99m human polyclonal IgG radiolabeled via the hydrazino nicotinamide derivative for imaging focal sites of infection in rats. *J Nucl Med* 1990;31:2022-2028.
19. Krecjarek GE, Tucker KL. Covalent attachment of chelating groups to macromolecules. *Biochem Biophys Res Commun* 1977;77:581-585.
20. Khaw BA, Mattis JA, Melincoff G, Strauss HW, Gold HK, Haber E. Imaging of experimental myocardial infarction. *Hybridoma* 1984;3:11-23.
21. Rubin RH, Fischman AJ, Callahan RJ, et al. The utility of  $^{111}\text{In}$ -labeled nonspecific immunoglobulin scanning in the detection of focal inflammation. *N Engl J Med* 1989;321:935-940.
22. Fischman AJ, Rubin RH, Khaw BA, et al. Detection of acute inflammation with  $^{111}\text{In}$ -labeled nonspecific polyclonal IgG. *Semin Nucl Med* 1988;18:335-344.
23. McAfee JG, Gagne GM, Subramanian G, et al. Distribution of leukocytes labeled with indium-111-oxine in dogs with acute inflammatory lesions. *J Nucl Med* 1980;21:1059-1068.
24. McAfee JG, Subramanian G, Gagne GM. Technique of leukocyte harvesting and labeling: problems and perspectives. *Semin Nucl Med* 1984;14:83-106.
25. Duncan DB. Multiple range tests and multiple F-tests. *Biometrics* 1955;11:1-42.
26. Babich JW, Barrow SA, Graham W, Fischman AJ. Infection imaging with technetium-99m chemotactic peptides in dogs. *J Nucl Med* 1995;36:230P.
27. Senda M, Fischman AJ, Weise S, Alpert NM, Correia JA, Rubin RH, Strauss HW. Evaluation of regional perfusion, oxygen metabolism, blood volume and permeability to IgG in experimental skeletal muscle infection in the rabbit. *Eur J Nucl Med* 1992;19:166-172.
28. Babich JW, Fischman AJ. Influence of coligand on the distribution of  $^{99m}\text{Tc}$ -labeled hydrazino nicotinamide derivatized chemotactic peptides in normal rats. *Nucl Med Biol* 1995;22:25-30.

## EDITORIAL

# Technetium-99m-Labeled Chemotactic Peptides: Specific for Imaging Infection?

In 1991, Fischman et al. (1) were the first to report the potential diagnostic use of  $^{111}\text{In}$ -labeled chemotactic peptide analogs of N-formyl-methionyl-leucyl-phenylalanine (ForMLF), a bacterial product for imaging infection. Subsequently, Babich et al. (2,3) reported that in the same rat model,  $^{99m}\text{Tc}$ -labeled hydrazinonicotinamide (HYNIC) derivatized chemotactic peptides also localize at the site of infection. They identified that N-formyl-methionyl-leucyl-phenylalanine-lysine (fMLFK) conjugated to HYNIC and labeled with  $^{99m}\text{Tc}$  had the most favorable distribution characteris-

tics for infection imaging. While these reports clearly documented the uptake of radiolabeled peptides at the infection site, the specificity of these tracers for infection and the exact mechanism(s) of localization are not well understood. It was assumed that the mechanism of uptake of chemotactic peptides in the infection/inflammation foci is mediated by high-affinity binding to For-MLF receptors on leukocytes.

In this issue, Babich et al. (4) and van der Laken et al. (5), report that  $^{99m}\text{Tc}$ -labeled chemotactic peptides specifically localize at the site of infectious foci in a rabbit model of acute infection. Despite the differences in experimental design, the two investigators studied the infection uptake and specificity of the same radiotracer, the

high-affinity chemotactic peptide agonist  $^{99m}\text{Tc}$ -fMLFK-HYNIC. While the results reported in these two articles are encouraging for further work, it is important to analyze the different lines of evidence presented here to demonstrate the in vivo specificity of  $^{99m}\text{Tc}$  peptides for infection.

Babich et al. (4) performed three studies in rabbits with E. Coli infection. The first compares the infection/background or target-to-background ratios (T/B) of  $^{99m}\text{Tc}$ -fMLFK-HYNIC with that of  $^{111}\text{In}$ -labeled DTPA, RBC and IgG. Since the RBCs and IgG remain in circulation longer than the peptide, T/B ratios are expected to be lower than the labeled peptides. Imaging studies at 2-3 hr, however, show that T/B ratios of all three tracers are between 2.0-3.0. The most striking difference is seen only at 16-18

Received May 2, 1997; accepted May 12, 1997.

For correspondence or reprints contact: Shankar Valabhajosula, PhD, Professor of Radiopharmacy in Radiology, Division of Nuclear Medicine, New York Hospital-Cornell University Medical College, 525 East 68th St., New York, NY 10021.